

## Supporting Information for

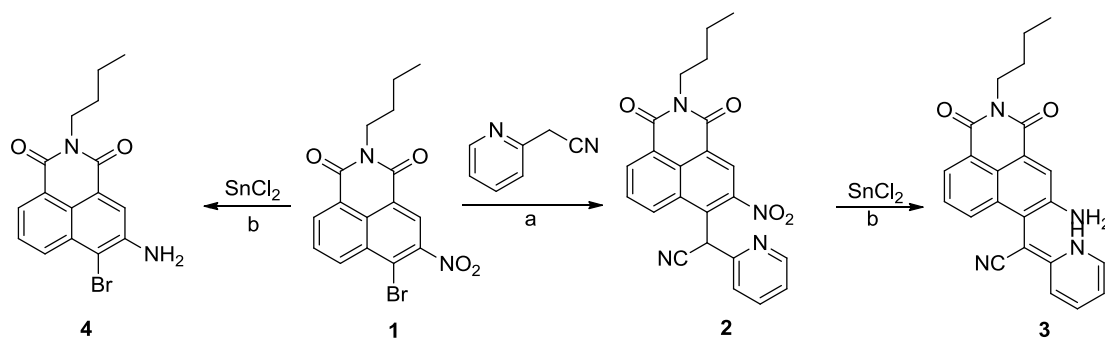
### Reversible and selective chemochemosensor based on intramolecular NH $\cdots$ NH $_2$ hydrogen bonding for cyanide and pH detection

Chuanxiu Zhang, Kai Ji, Xinyu Wang, Hongwei Wu and Chuanxiang Liu\*

School of Chemical and Environmental Engineering, Shanghai Institute of  
Technology, 201418 Shanghai, China

**e-mail: cxliu@sit.edu.cn;**

1. $^1\text{H}$ , $^{13}\text{C}$ NMR, IR and HRMS-ESI copies of the compound <b>2</b> (Fig.S1-S4).....	S3
2. $^1\text{H}$ , $^{13}\text{C}$ NMR, IR and HRMS-ESI copies of the compound <b>3</b> (Fig.S5-S8).....	S5
3. $^1\text{H}$ , $^{13}\text{C}$ NMR, IR and HRMS-ESI copies of the compound <b>4</b> (Fig.S9-S12).....	S8
4. The $^1\text{H}$ NMR spectra of compound <b>3</b> and <b>4</b> (Fig.S13).....	S10
5. The $I_{\text{max}}$ of chemosensor <b>3</b> in various polar solvents (Fig.S14).....	S11
6. DFT calculation for chemosensor <b>3</b> (Fig.S15).....	S12
7. UV-visible spectra of chemosensor <b>3</b> (Fig.S16) .....	S12
8. The UV detection limit of the chemosensor <b>3</b> with $\text{CN}^-$ in DMSO (Fig.S17).....	S13
9. The UV detection limit of the chemosensor <b>3</b> with $\text{CN}^-$ in DMSO/H $_2\text{O}$ (Fig.S18) .....	S14
10. The UV detection limit of the chemosensor <b>3</b> with $\text{CN}^-$ in H $_2\text{O}$ (Fig.S19).....	S15
11. UV-visible spectra of chemosensor <b>3</b> in the presence of different anions in H $_2\text{O}$ (Fig.S20). ..	S16
12. Interference experiments of chemosensor <b>3</b> toward cyanide in H $_2\text{O}$ (Fig.S21).....	S17
13. The response time of chemosensor <b>3</b> to $\text{CN}^-$ in aqueous media (Fig.S22).....	S17
14. Fluorescence spectra of chemosensor <b>3</b> in the presence of different cations in H $_2\text{O}$ (Fig.S23) .....	S18
15. Linear fluorescence response of chemosensor <b>3</b> to $\text{CN}^-$ in DMSO/H $_2\text{O}$ (Fig.S24).....	S19
16. The fluorescence detection limit of the chemosensor <b>3</b> with $\text{CN}^-$ in DMSO (Fig.S25). .....	S19
17. The fluorescence detection limit of the chemosensor <b>3</b> with $\text{CN}^-$ in DMSO/H $_2\text{O}$ (Fig.S26) ..	S20
18. The fluorescence detection limit of the chemosensor <b>3</b> with $\text{CN}^-$ in H $_2\text{O}$ (Fig.S27).....	S21
19. The $^1\text{H}$ NMR spectra of the chemosensor <b>3</b> with $\text{CN}^-$ in DMSO- $d_6$ (Fig.S28).....	S22
20. The $^1\text{H}$ NMR spectra of the chemosensor <b>3</b> with $\text{F}^-$ in DMSO- $d_6$ (Fig.S29).....	S22
21. Confocal microscopic images of Hela cells (Fig.S30).....	S23
22. Fluorescence spectra of chemosensor <b>3</b> at different pH values in DMSO/H $_2\text{O}$ (Fig.S31).....	S23
23. Fluorescence spectra of chemosensor <b>3</b> at different pH values in H $_2\text{O}$ (Fig.S32). .....	S24



**Scheme S1.** Synthesis of chemosensor **3** and its cartoon-type representation; Reagents and conditions: (a) NaH, N<sub>2</sub>, THF, 2-(cyanomethyl)pyridine, r.t., 70% yield; (b) SnCl<sub>2</sub>, r.t., 79% yield.

### Materials and instruments

Unless otherwise noted, solvents and reagents were analytical grade and used without further purification. THF were distilled from Na prior to use. UV-visible absorption spectra were obtained on a SHIMADZU UV-1800 spectrophotometer. Fluorescence emission spectra were obtained on a Hitach F-4600 Fluorescence spectrophotometer. IR were recorded on NICOLET 6700 FT-IR. NMR spectra were recorded on Bruker AVANCE III 500 MHz (500 MHz for <sup>1</sup>H) or Bruker AM-400 spectrometer (100 MHz for <sup>13</sup>C NMR), and chemical shifts were reported in parts per million (ppm, δ) downfield from internal standard Me<sub>4</sub>Si (TMS). Multiplicities of signals are described as follows: s --- singlet, br. s --- broad singlet, d --- doublet, t --- triplet, m --- multiplet. Coupling constants were reported in hertz (Hz). HRMS were recorded on solanX 70 FT-MS spectrometer with methanol and water (v/v = 1:1) as solvent.

**N-butyl-4-bromo-3-nitro-1,8-naphthalimide (1)** was synthesized according to the literature reported procedure<sup>1</sup>.

**Synthesis of 2-(N-butyl-3-nitro-1,8-naphthalimide)-2-(pyridin-2-yl)acetonitrile (2):** To a solution of NaH (60% in oil) (1.60 g, 40 mmol) in 30 mL anhydrous THF was added 2-cyanomethylpyridine (0.70 g, 5.60 mmol) under N<sub>2</sub> at room temperature, after 30 min the mixture was then added **1** (1.50 g, 4 mmol). The reaction mixture was stirred at room temperature for another 2 h. After the reaction was completed, the reaction mixture was quenched with a mixture of saturated ammonium chloride solution and hydrochloric acid (2N). The anhydrous solution was extracted with EA (25 mL × 3). The organic layer was dried with anhydrous sodium sulfate, concentrated and purified by column chromatography eluting with PE/EA (5:1) to give **2** (1.12 g, 70%) as a black solid with a mp of 137–138 °C. <sup>1</sup>H NMR (500 MHz, CDCl<sub>3</sub>) δ 8.94 (s, 1H), 8.65 (d, *J* = 7.5 Hz, 1H), 8.58 (d, *J* = 8.5 Hz, 1H), 8.46 (d, *J* = 4.0 Hz, 1H), 7.78 (dd, *J*<sub>1</sub> = 7.0, *J*<sub>2</sub> = 9.0 Hz 1H), 7.70 (dd, *J* = 8.0, *J* = 7.5 Hz, 1H), 7.50 (d, *J* = 8.0 Hz, 1H), 7.23-7.20 (m, 1H), 6.60 (s, 1H), 4.12 (t, *J* = 7.5 Hz, 2H), 1.67-1.61 (m, 2H), 1.38-1.34 (m, 2H), 0.91 (t, *J* = 7.5 Hz, 3H); <sup>13</sup>C NMR (100 MHz, DMSO-*d*<sub>6</sub>) δ 13.7, 19.9, 29.8, 94.8, 98.9, 109.6, 112.7, 116.0, 120.5, 122.0, 123.5, 127.1, 128.7, 136.6, 136.8, 147.2, 149.2, 150.3, 154.2, 154.7, 163.6, 163.9; IR (KBr) 3080, 2959, 2873, 2157, 1712, 1680, 1597, 1586, 1466, 1435, 1435, 1355, 1277, 1233, 1112, 995, 803, 790, 761 cm<sup>-1</sup>; HRMS-ESI (m/z): [M+H]<sup>+</sup> (calcd for C<sub>23</sub>H<sub>19</sub>N<sub>4</sub>O<sub>4</sub>) 415.14063; Found 415.14214.

**Synthesis of (E)-2-(5-amino-2-butyl-1,3-dioxo-2,3-dihydro-1H-benzo[de]isoquinolin-6-yl)-2-(pyridin-2(1H)-ylidene)acetonitrile (3):**

**2** (0.15 g, 0.36 mmol) and SnCl<sub>2</sub> (0.60 g, 3.20 mmol) were dissolved in (20 mL) EA, the reaction mixture was stirred under N<sub>2</sub> at room temperature for 1 h. After the reaction was completed, the solution was filtered and saturated Na<sub>2</sub>CO<sub>3</sub> (aq) (150 mL) was then added. The resulting suspension was then extracted with ethyl acetate, washed with brine, and dried over anhydrous

sodium sulfate, concentrated and purified by column chromatography eluting with PE/EA (2:1) to give **3** (0.11 g, 79%) as a red solid with a mp of 218–220 °C. <sup>1</sup>H NMR (500 MHz, DMSO-*d*<sub>6</sub>) δ 12.17 (s, 1H), 8.70 (d, *J* = 4.5 Hz, 1H), 8.61 (d, *J* = 8.0 Hz, 1H), 8.31 (s, 1H), 8.31 (d, *J* = 6.5 Hz, 1H), 7.87 (dd, *J*<sub>1</sub> = 8.0, *J*<sub>2</sub> = 7.5 Hz, 1H), 7.67 (d, *J* = 7.5 Hz, 1H), 7.52 (dd, *J*<sub>1</sub> = *J*<sub>2</sub> = 8.0 Hz, 1H), 7.29 (dd, *J*<sub>1</sub> = 5.5, *J*<sub>2</sub> = 6.5 Hz, 1H), 6.87 (s, 2H), 4.06 (t, *J* = 7.5 Hz, 2H), 1.66–1.60 (m, 2H), 1.40–1.35 (m, 2H), 0.94 (t, *J* = 7.5 Hz, 3H); <sup>13</sup>C NMR (100 MHz, DMSO-*d*<sub>6</sub>) δ 13.6, 19.7, 29.5, 109.5, 113.6, 118.7, 121.7, 122.9, 125.6, 128.8, 129.3, 131.1, 132.7, 133.2, 136.6, 138.2, 147.4, 149.3, 153.1, 153.2, 162.0, 162.7; IR (KBr) 3445, 2957, 2926, 2856, 2375, 1681, 1652, 1500, 1463, 1427, 1384, 1233, 1166, 1092, 810, 776, 607 cm<sup>-1</sup>; HRMS-ESI (*m/z*): [M+H]<sup>+</sup> (calcd for C<sub>23</sub>H<sub>21</sub>N<sub>4</sub>O<sub>2</sub>) 385.16645; Found 385.16645.

**Synthesis of N-butyl-4-bromo-3-amino-1,8-naphthalimide (4):** **2** (0.15 g, 0.40 mmol) were dissolved in a mixture of ethyl acetate (20 mL) and THF (10 mL), warmed to 70 °C and under N<sub>2</sub>. SnCl<sub>2</sub> (0.60 g, 3.20 mmol) was then added and the reaction mixture was stirred for 2 hours at 70 °C. After cooling, the solution was filtered and saturated Na<sub>2</sub>CO<sub>3</sub> (aq) (150 mL) was then added. The resulting suspension was then extracted with ethyl acetate, washed with brine, and dried over anhydrous sodium sulfate, concentrated and purified by column chromatography eluting with PE/EA (15:1) to give **4** (0.10 g, 72%) as a yellow solid with a mp of 192–193 °C. <sup>1</sup>H NMR (500 MHz, DMSO-*d*<sub>6</sub>) δ 8.24 (d, *J* = 8.5 Hz, 1H), 8.18 (d, *J* = 7.0 Hz, 1H), 8.13 (s, 1H), 8.79 (dd, *J*<sub>1</sub> = 8.0, *J*<sub>2</sub> = 7.5 Hz, 1H), 6.34 (s, 2H), 4.01 (t, *J* = 7.5 Hz, 2H), 1.63–1.57 (m, 2H), 1.39–1.31 (m, 2H), 0.92 (t, *J* = 7.5 Hz, 3H); <sup>13</sup>C NMR (100 MHz, DMSO-*d*<sub>6</sub>) δ 13.7, 19.8, 29.6, 106.6, 121.1, 121.7, 121.8, 122.1, 125.7, 128.2, 129.7, 131.4, 145.2, 162.9, 163.2; IR (KBr) 3323, 2961, 1694, 1650, 1618, 1420, 1339, 1285, 1231, 1078, 778, 749; HRMS-ESI (*m/z*): [M+H]<sup>+</sup> (calcd for C<sub>16</sub>H<sub>16</sub>BrN<sub>2</sub>O<sub>2</sub>) 347.03952; Found 347.03742.

**Typical procedure of NMR titration of 3 with cyanide ions:** <sup>1</sup>H NMR titrations (500 MHz) were performed with a DMSO-*d*<sub>6</sub> solution of **3** (0.04 mol L<sup>-1</sup>, 0.5 mL) and a DMSO-*d*<sub>6</sub> solution of TBACN (1.5 mol L<sup>-1</sup>). The TBACN solution was introduced in portions (7, 14, 28, 42, 70 and 126 μL; 14 μL corresponds to 1.0 equiv) and, after every addition, the solution was maintained for 1 min at 298K.

## References

[1] a) J. Yeow, A. Kaur, M. D. Anscomb, E. J. New, *Chem. Commun.* **2014**, 50, 8181–8184; b) X. Zeng, X. Zhang, B. Zhu, H. Jia, Y. Li, *Dyes and Pigments* **2012**, 94, 10–15.

1.  $^1\text{H}$ ,  $^{13}\text{C}$  NMR, IR and HRMS-ESI copies of the compound 2.

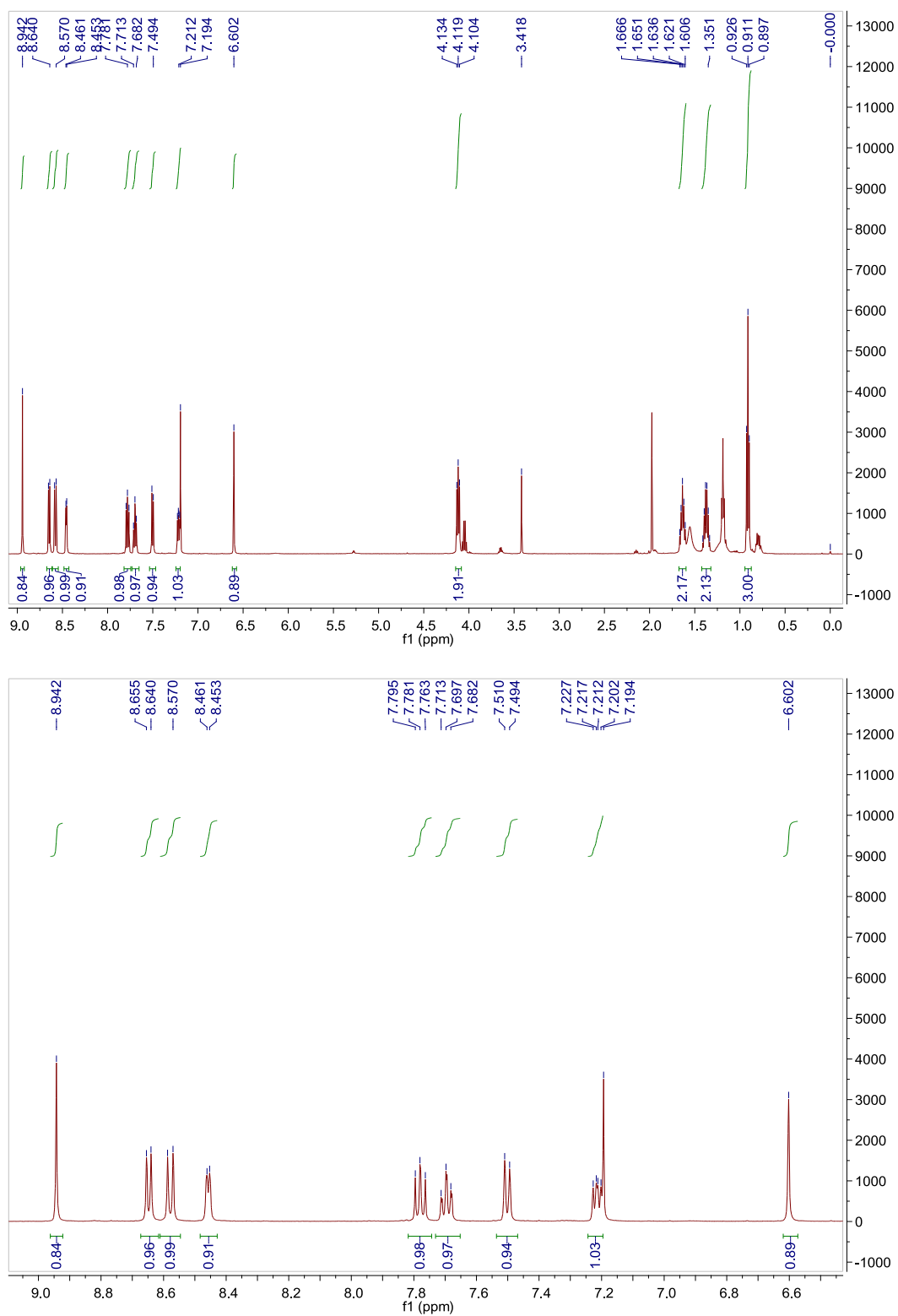


Fig. S1.  $^1\text{H}$  NMR ( $\text{CDCl}_3$ , 500 MHz) spectra of compound 2.

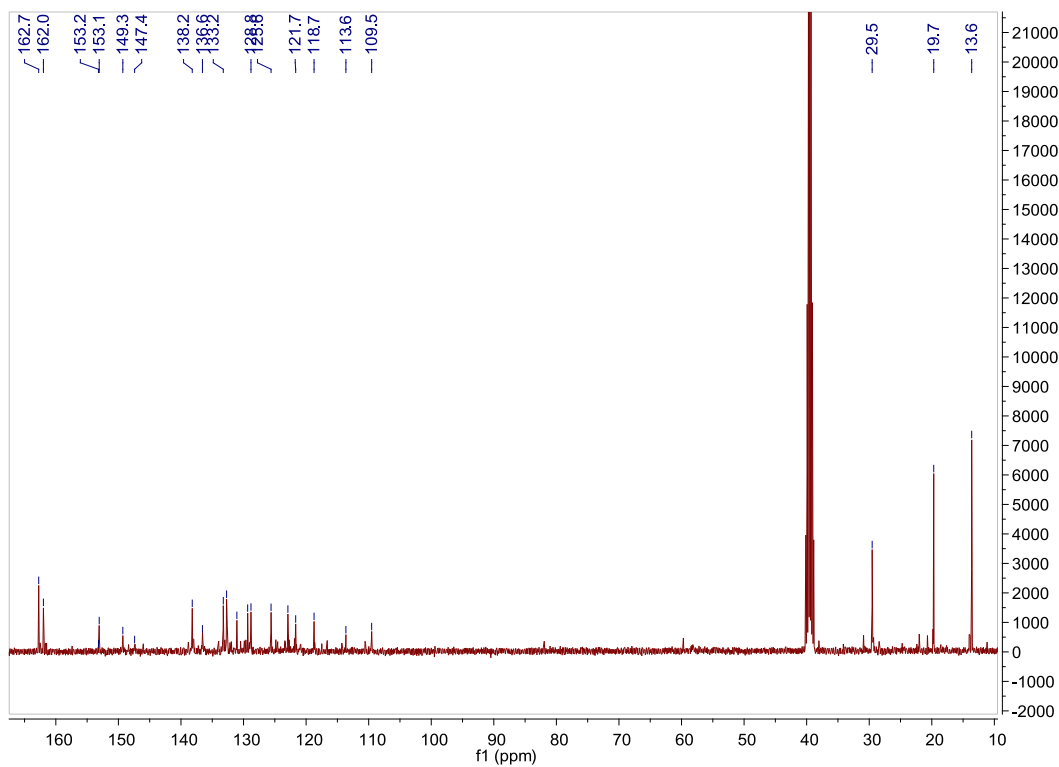


Fig. S2.  $^{13}\text{C}$  NMR (DMSO- $d_6$ , 100 MHz) spectra of compound 2.

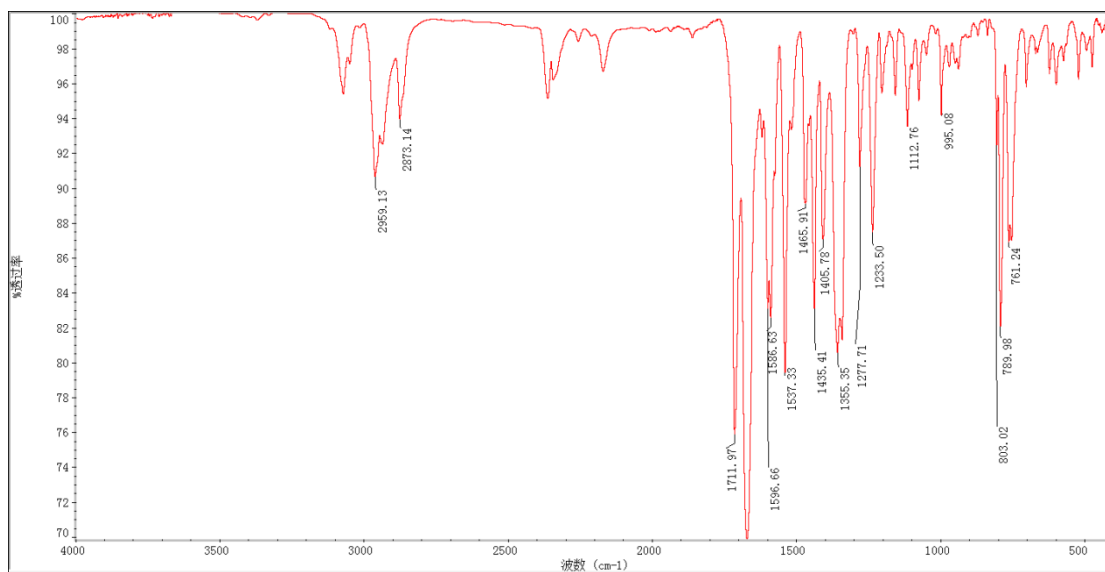
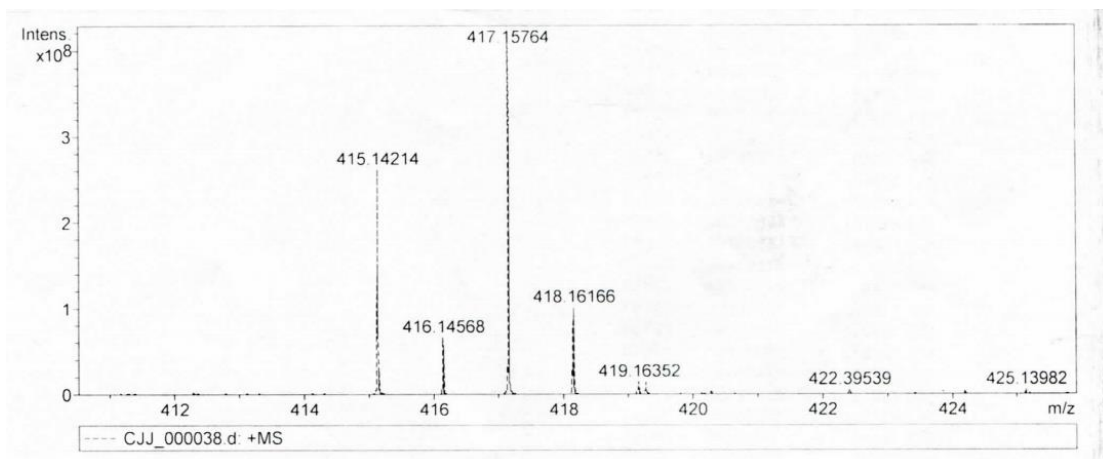
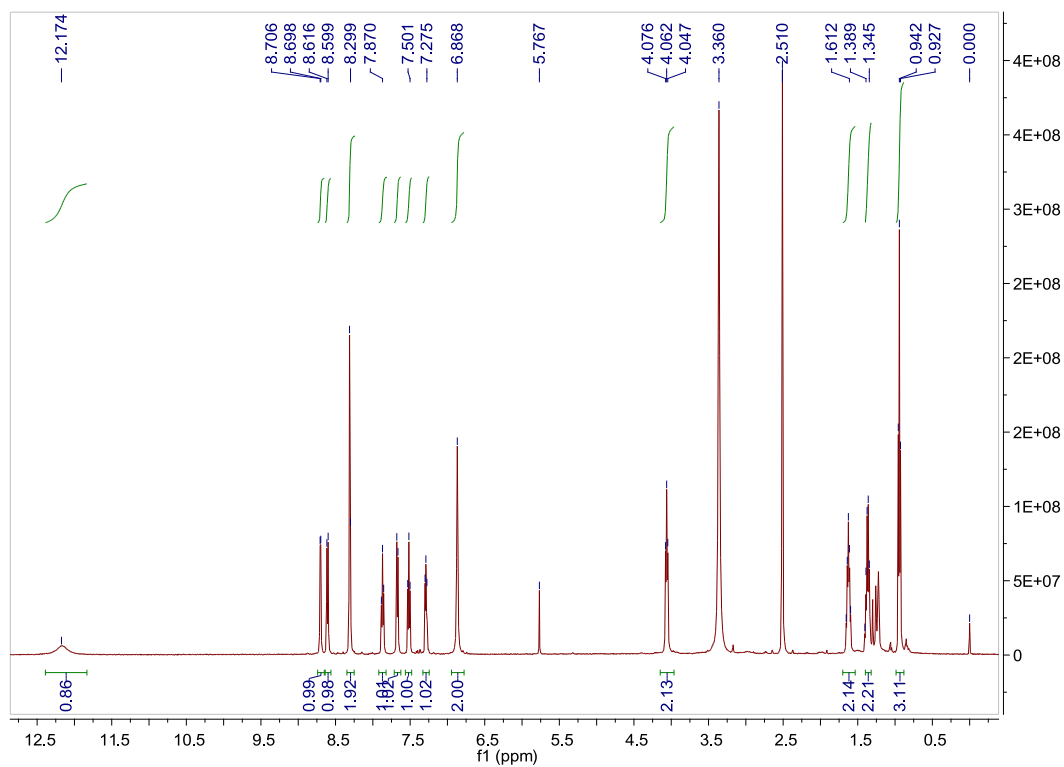


Fig. S3. IR spectra of compound 2.



**Fig. S4.** ESI mass spectra of compound 2.

**2.  $^1\text{H}$ ,  $^{13}\text{C}$  NMR, IR and HRMS-ESI copies of the compound 3.**



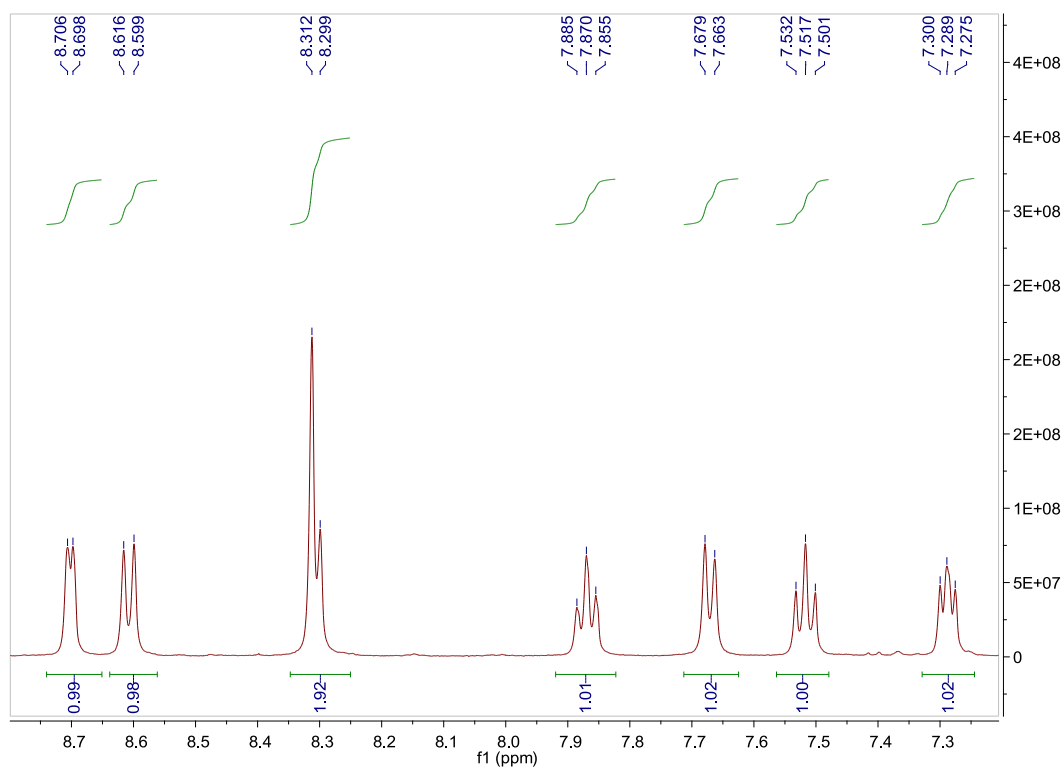


**Fig. S5.**  $^1\text{H}$  NMR (DMSO- $d_6$ , 500 MHz) spectra of compound **3**.

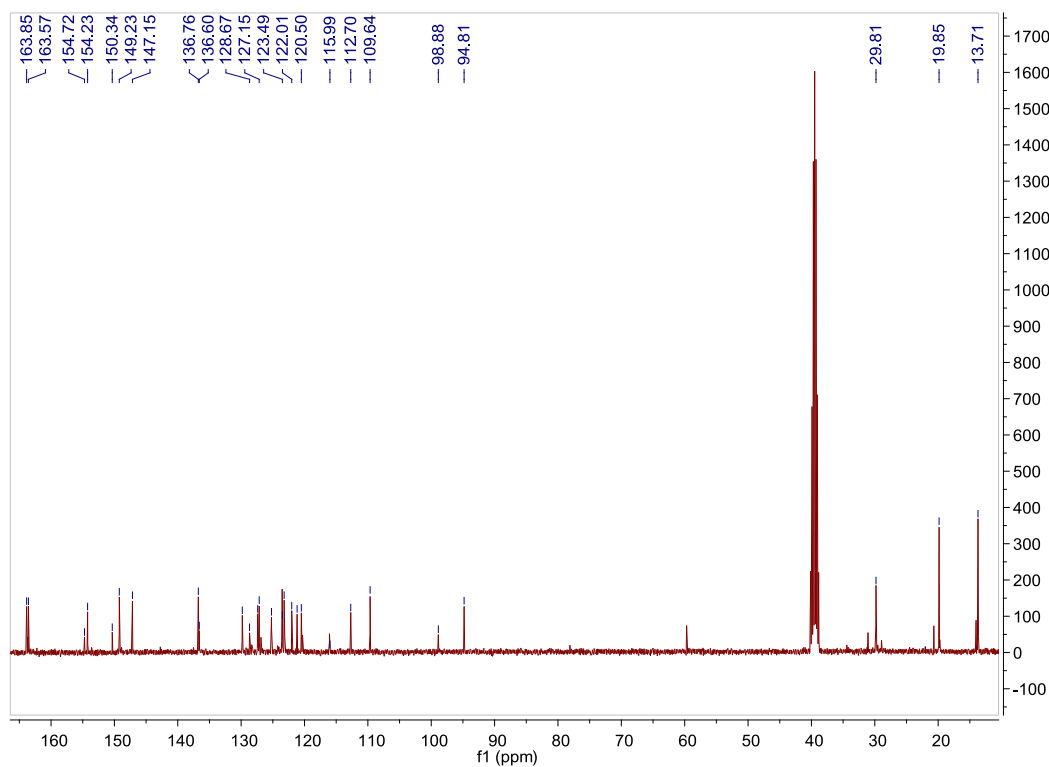


**Fig. S6.**  $^{13}\text{C}$  NMR (DMSO- $d_6$ , 100 MHz) spectra of compound **3**.

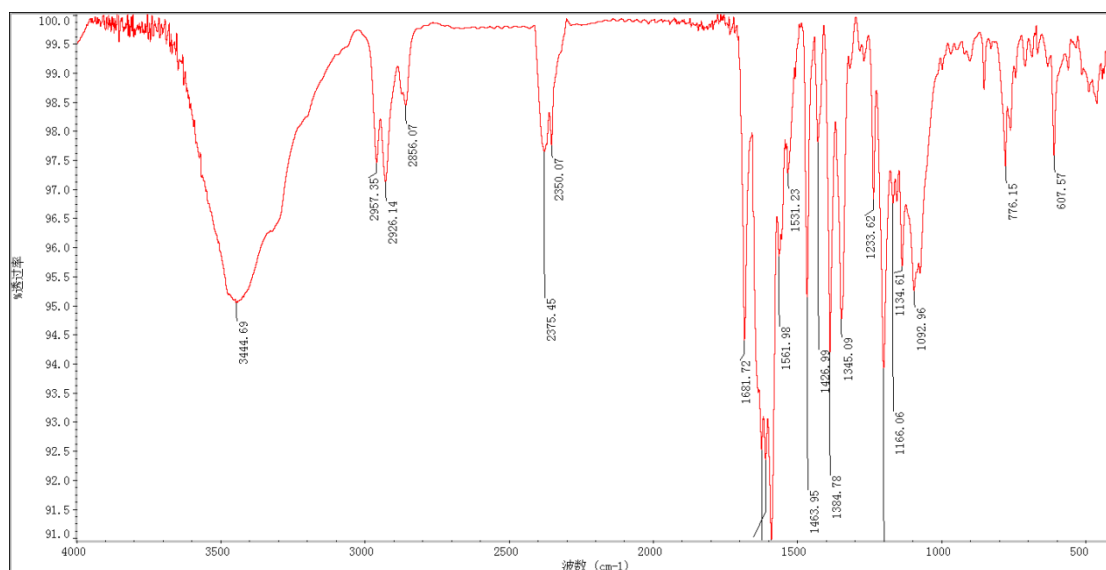


**Fig. S7.** IR spectra of compound **3**.

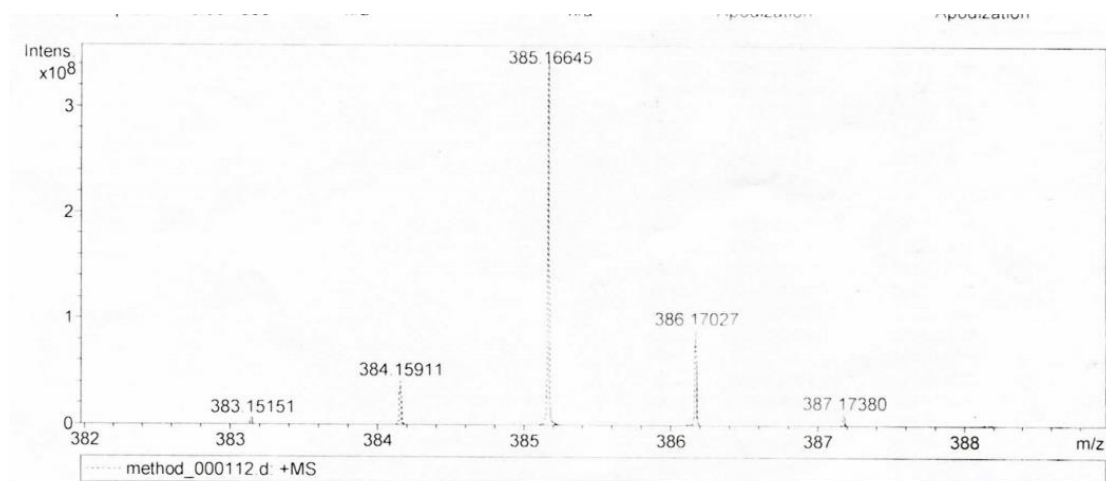


**Fig. S8.** ESI mass spectra of compound **3**.



3.  $^1\text{H}$ ,  $^{13}\text{C}$  NMR, IR and HRMS-ESI copies of the compound 4.

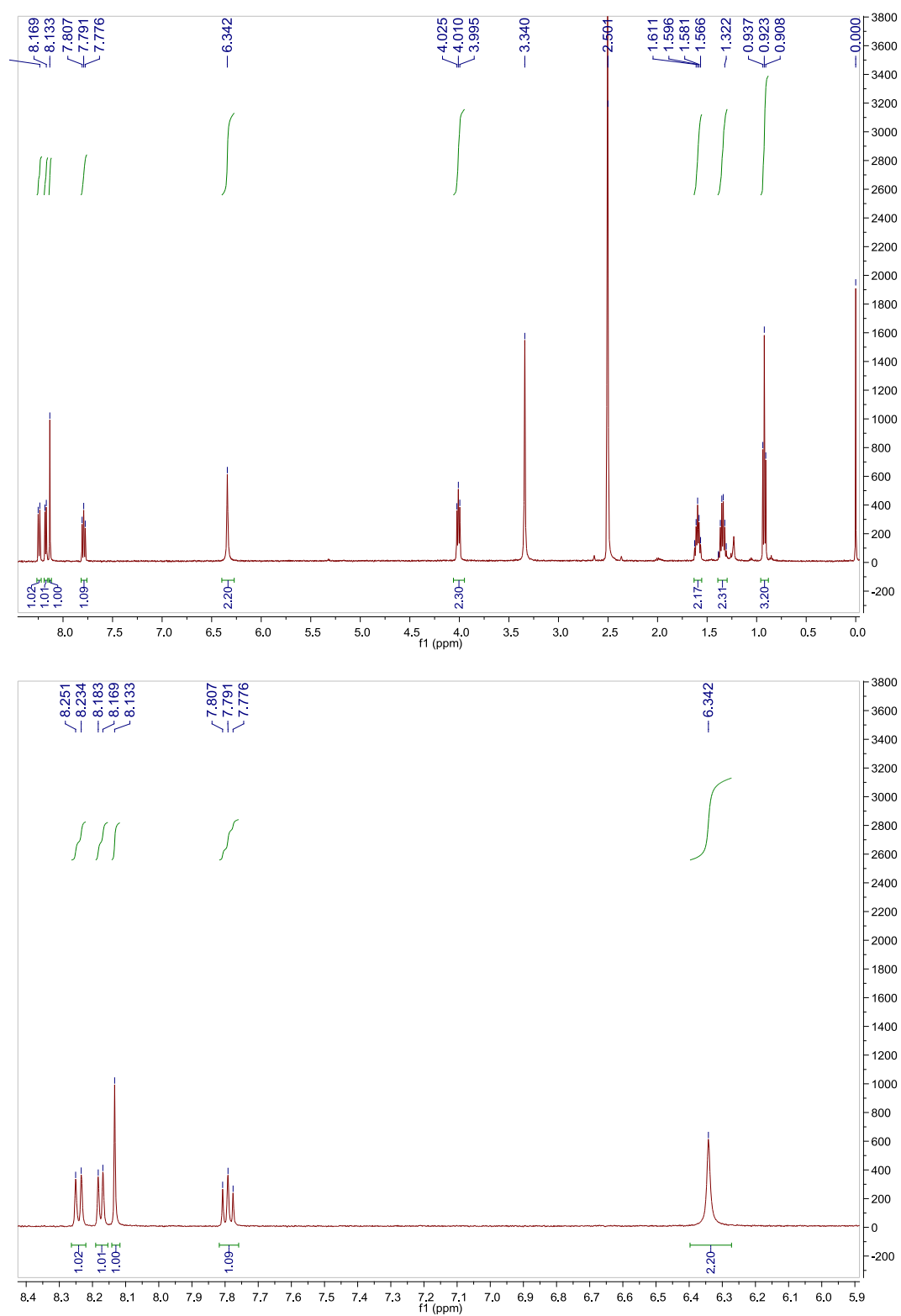
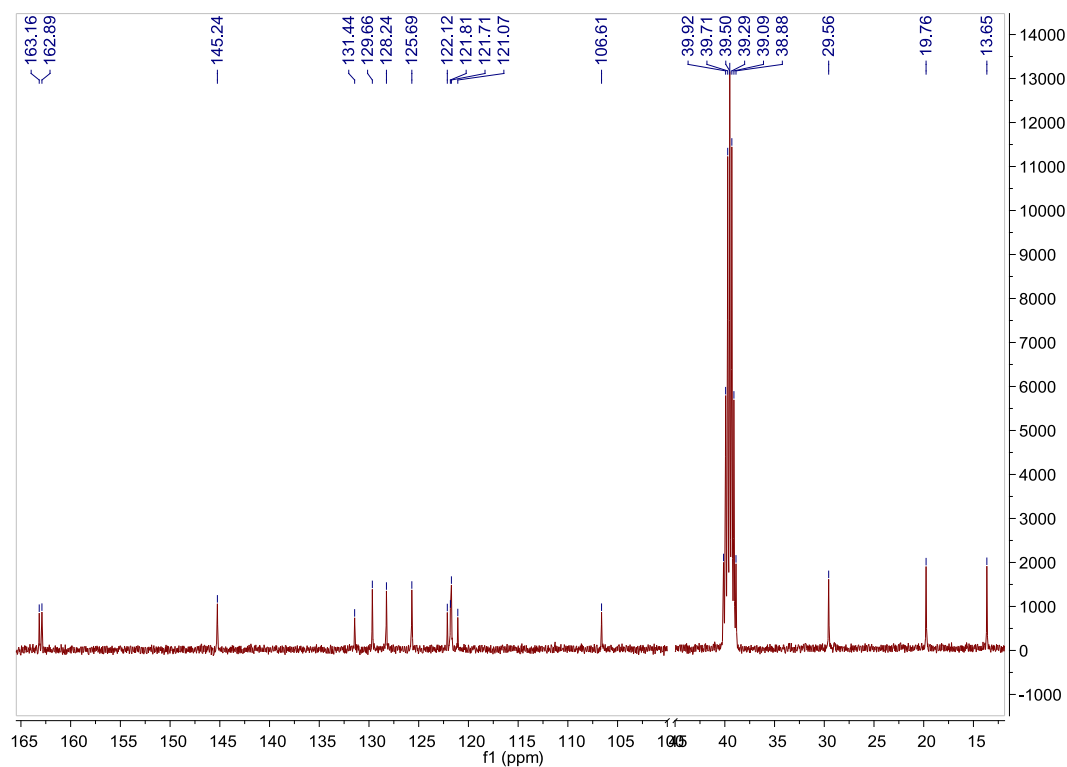
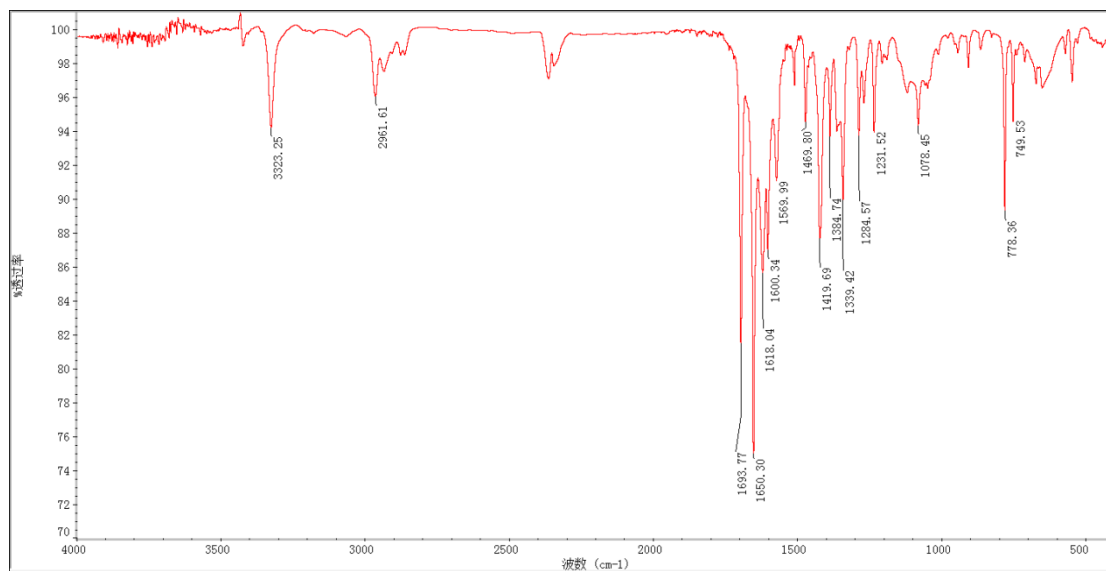


Fig. S9.  $^1\text{H}$  NMR ( $\text{DMSO-}d_6$ , 500 MHz) spectra of compound 4.



**Fig. S10.**  $^{13}\text{C}$  NMR (DMSO- $d_6$ , 100 MHz) spectra of compound **4**.



**Fig. S11.** IR spectra of compound **4**.

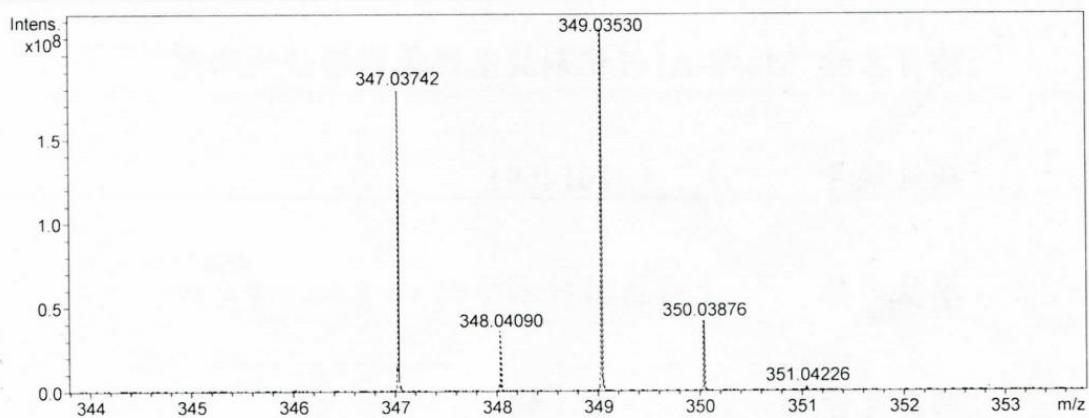


**Fig. S12.** ESI mass spectra of compound 4.

**4. The <sup>1</sup>H NMR spectra of compound 3 and 4**

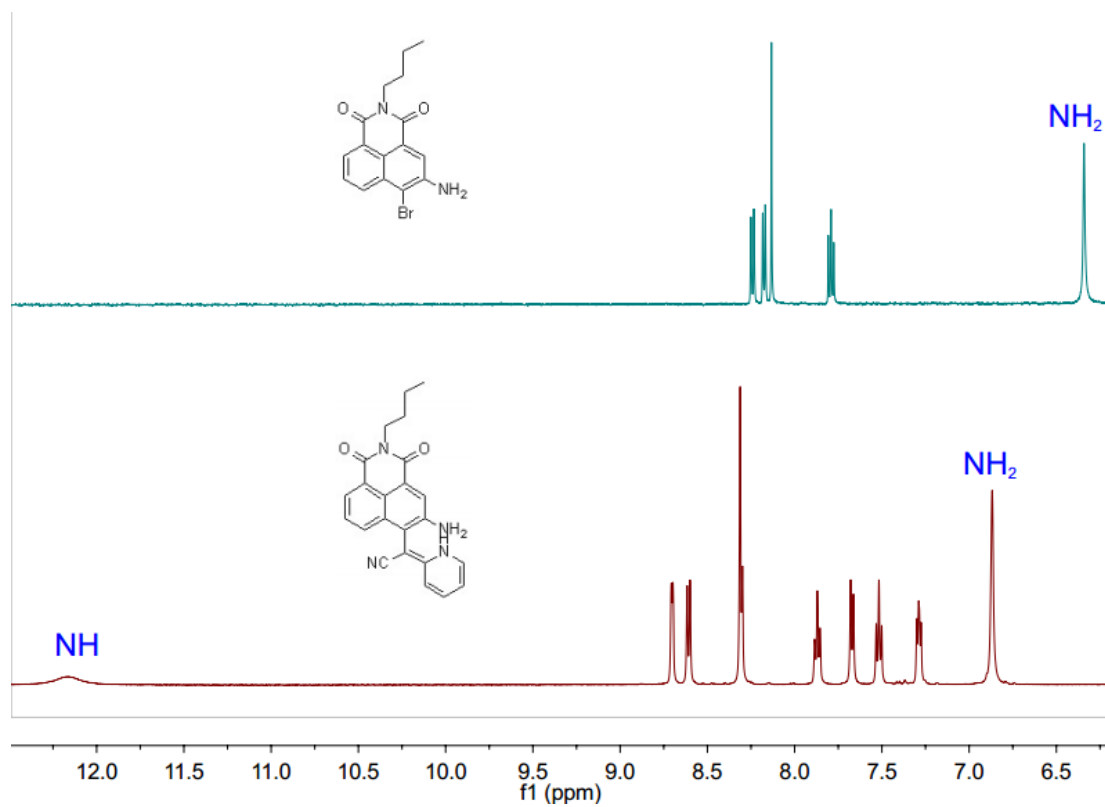


**Fig. S13.** <sup>1</sup>H NMR (DMSO-*d*<sub>6</sub>, 500 MHz) spectra of compound 3 and 4.

5. The  $I_{\max}$  of chemosensor **3** in various polar solvents

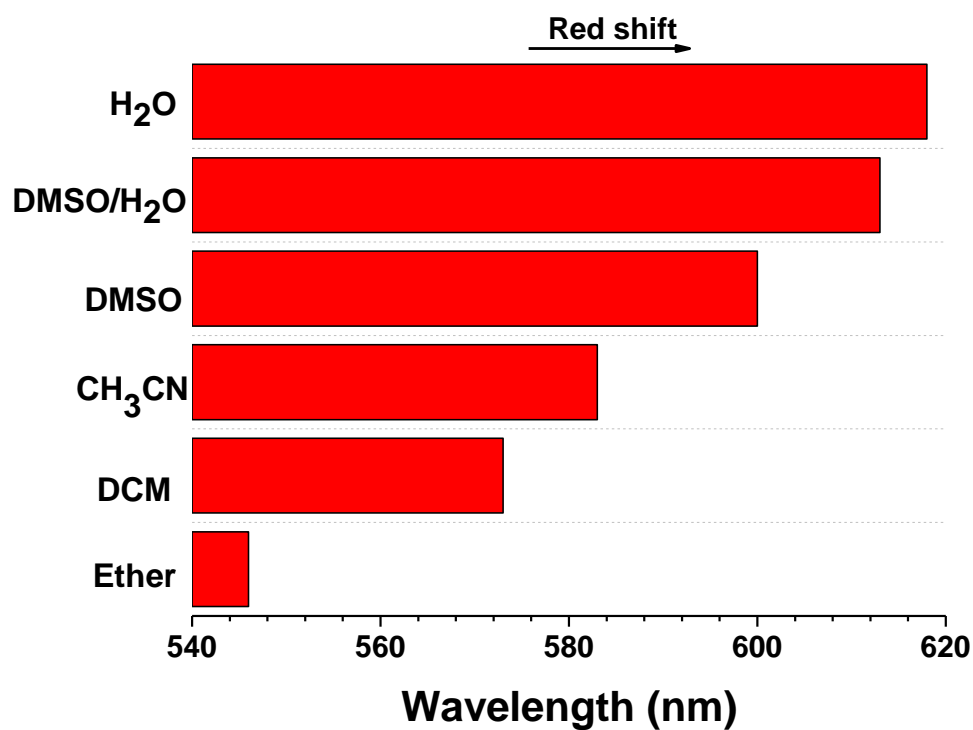


**Fig. S14.** The fluorescent maximum emission wavelength of chemosensor **3** in diethyl ether, dichloromethane, acetonitrile, dimethyl sulfoxide, dimethyl sulfoxide/water (1:1, v/v), and water. Excitation at 480 nm.

## 6. DFT calculation for chemosensor **3**

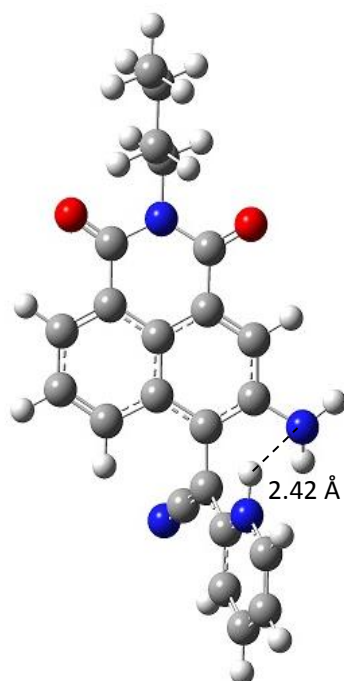


**Fig. S15.** The optimized structure of chemosensor **3** at the level of M06-2X functional with 6-31+G (d, p) basis set.

## 7. UV-visible spectra of chemosensor **3**

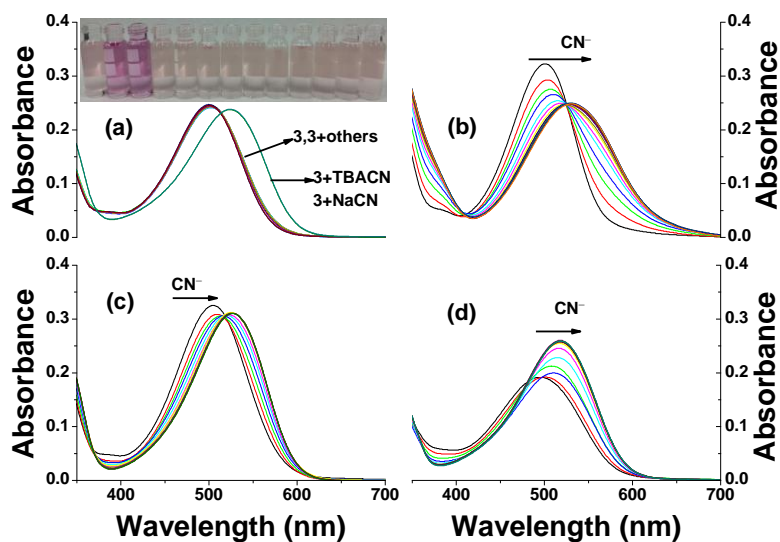


**Fig. S16.** UV-visible spectral changes of  $20 \mu\text{mol L}^{-1}$  solution of **3** (a) in DMSO/H<sub>2</sub>O (1:1) with various anions (4.0 equiv) (Inset: from left to right: **3** only, NaCN, TBACN, F<sup>-</sup>, AcO<sup>-</sup>, H<sub>2</sub>PO<sub>4</sub><sup>-</sup>, Cl<sup>-</sup>, Br<sup>-</sup>, I<sup>-</sup>, NO<sub>3</sub><sup>-</sup>, BF<sub>4</sub><sup>-</sup>, ClO<sub>4</sub><sup>-</sup>); (b) in DMSO (1.5 equiv); (c) in DMSO/H<sub>2</sub>O (1:1) (4.0 equiv); and (d) in H<sub>2</sub>O (10.0 equiv) upon titration with TBACN.

8. The UV detection limit of the chemosensor **3** with  $\text{CN}^-$  in DMSO

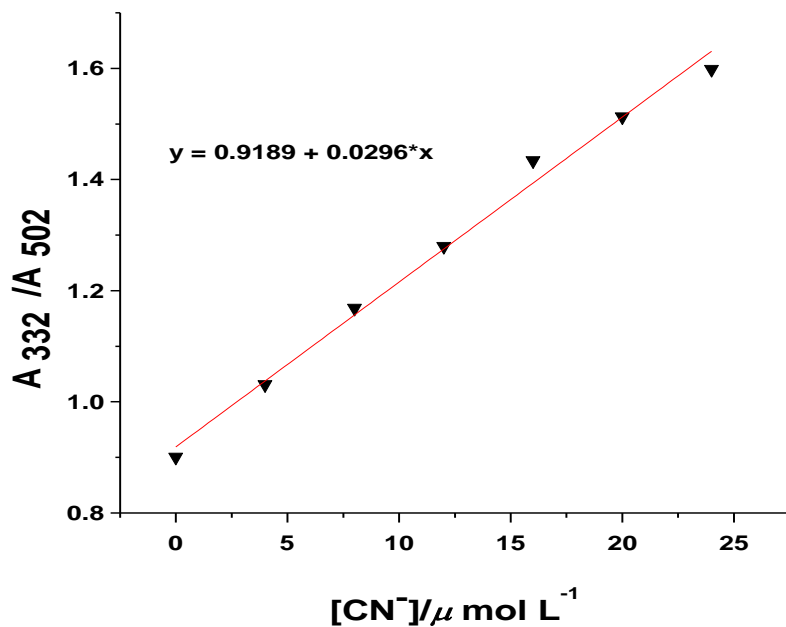


**Fig. S17.** Absorbance intensity ratio ( $A_{332}/A_{502}$ ) of chemosensor **3** ( $20 \mu\text{mol L}^{-1}$ ) as a function of  $\text{CN}^-$  concentration from  $0$ – $24 \mu\text{mol L}^{-1}$  ( $0$ – $1.2$  equiv) in DMSO.

SD	N
0.02548	7

The result of the analysis as follows:

Linear Equation:  $y = 0.9189 + 0.0296 * x$ ,  $R^2 = 0.9902$

$S = 2.96 * 10^4$ ,  $K = 3$ ,  $\delta = 0.02548$

$\text{LOD} = K * \delta/S = 2.58 \mu\text{mol L}^{-1}$

9. The UV detection limit of the chemosensor **3** with CN<sup>-</sup> in DMSO/H<sub>2</sub>O

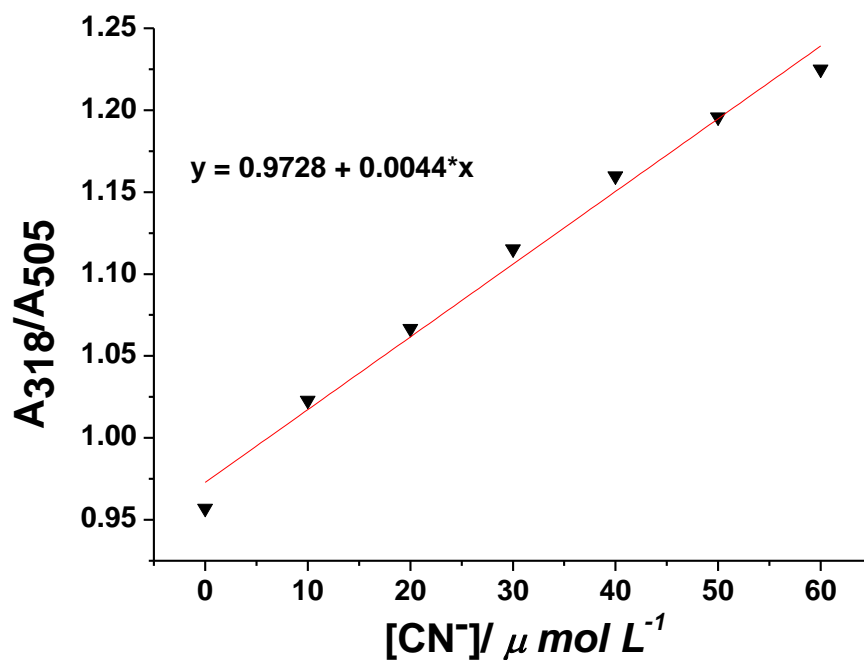


**Fig. S18.** Absorbance intensity ratio ( $A_{318}/A_{505}$ ) of chemosensor **3** ( $20 \mu\text{mol L}^{-1}$ ) as a function of CN<sup>-</sup> concentration from 0-60  $\mu\text{mol L}^{-1}$  (0-3.0 equiv) in DMSO/H<sub>2</sub>O (1:1, v/v).

SD	N
0.0117	7

The result of the analysis as follows:

Linear Equation:  $y = 0.9728 + 0.0044 * x$ ,  $R^2 = 0.98531$

$S = 4.4 * 10^3$ ,  $K = 3$ ,  $\delta = 0.0117$

$\text{LOD} = K * \delta/S = 7.98 \mu\text{mol L}^{-1}$

10. The UV detection limit of the chemosensor **3** with  $\text{CN}^-$  in  $\text{H}_2\text{O}$

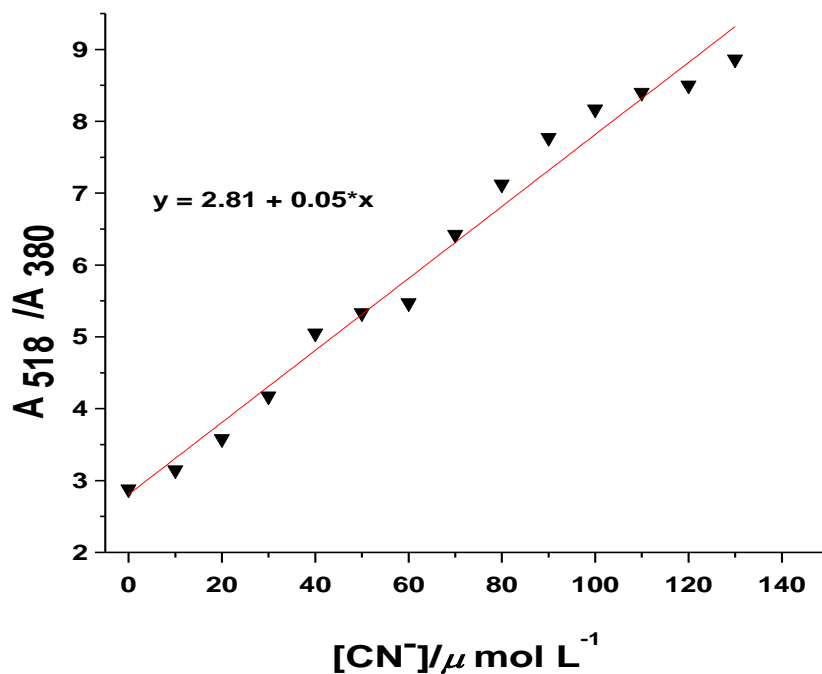


**Fig. S19.** Absorbance intensity ratio ( $A_{518}/A_{380}$ ) of chemosensor **3** ( $20 \mu\text{mol L}^{-1}$ ) as a function of  $\text{CN}^-$  concentration from  $0\text{--}130 \mu\text{mol L}^{-1}$  ( $0\text{--}6.5$  equiv).

SD	N
0.29351	14

The result of the analysis as follows:

Linear Equation:  $y = 2.81 + 0.05 * x$ ,  $R^2 = 0.98073$

$S = 5 * 10^4$ ,  $K = 3$ ,  $\delta = 0.29351$

$\text{LOD} = K * \delta/S = 17.61 \mu\text{mol L}^{-1}$



11. UV-visible spectra of chemosensor **3** in the presence of different anions in H<sub>2</sub>O.

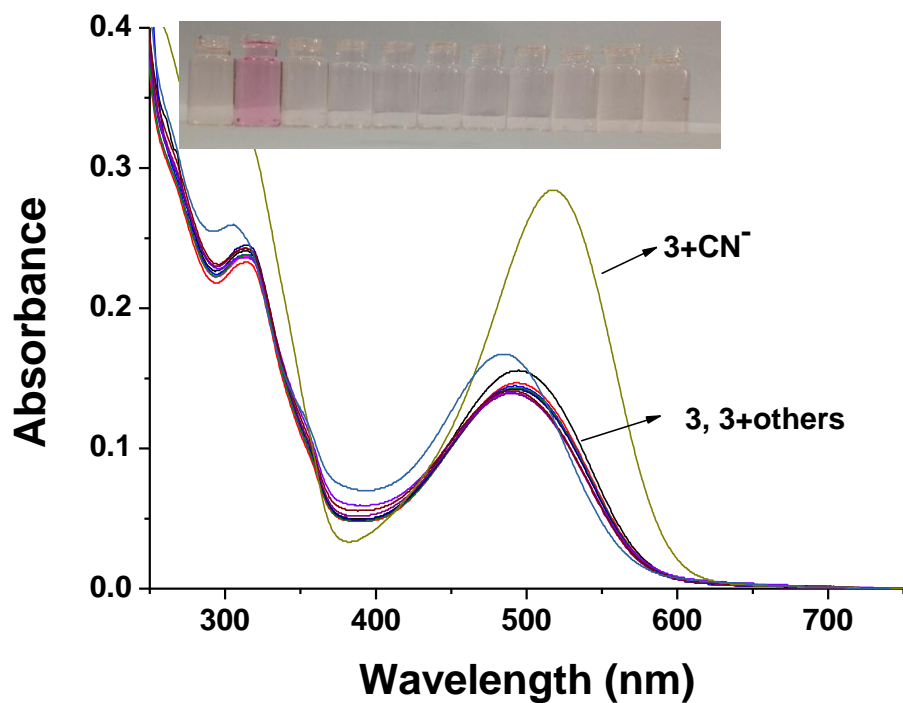


**Fig. S20.** UV-visible spectra of chemosensor **3** (20 μmol L<sup>-1</sup>) in the presence of different anions (ca. 10.0 equiv) in H<sub>2</sub>O; Color change of chemosensor **3** with different anions (from left to right: **3** only, CN<sup>-</sup>, F<sup>-</sup>, AcO<sup>-</sup>, H<sub>2</sub>PO<sub>4</sub><sup>-</sup>, Cl<sup>-</sup>, Br<sup>-</sup>, I<sup>-</sup>, NO<sub>3</sub><sup>-</sup>, BF<sub>4</sub><sup>-</sup>, ClO<sub>4</sub><sup>-</sup>).

12. Interference experiments of chemosensor **3** toward cyanide in H<sub>2</sub>O.

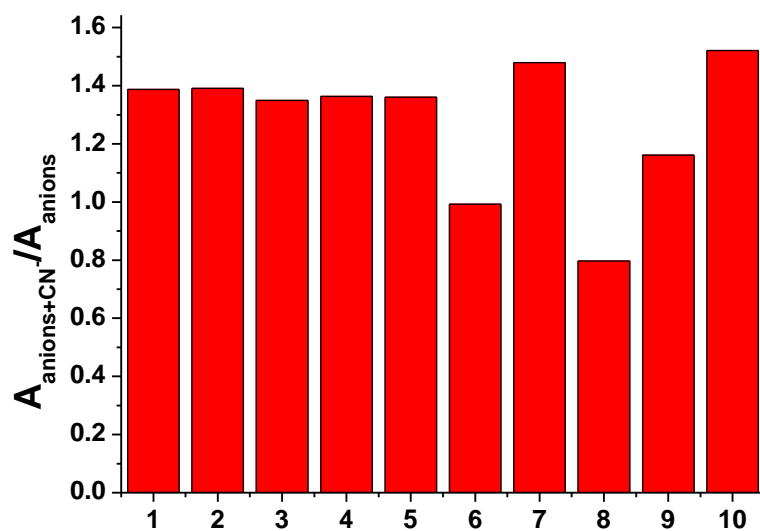


**Fig. S21.** Absorbance intensity ratio of chemosensor **3** toward cyanide and other anions (10.0 equiv, from left to right: H<sub>2</sub>PO<sub>4</sub><sup>-</sup>, Cl<sup>-</sup>, Br<sup>-</sup>, I<sup>-</sup>, NO<sub>3</sub><sup>-</sup>, HSO<sub>4</sub><sup>-</sup>, BF<sub>4</sub><sup>-</sup>, AcO<sup>-</sup>, ClO<sub>4</sub><sup>-</sup>, F<sup>-</sup>) in H<sub>2</sub>O.

13. The response time of chemosensor **3** to CN<sup>-</sup> in aqueous media

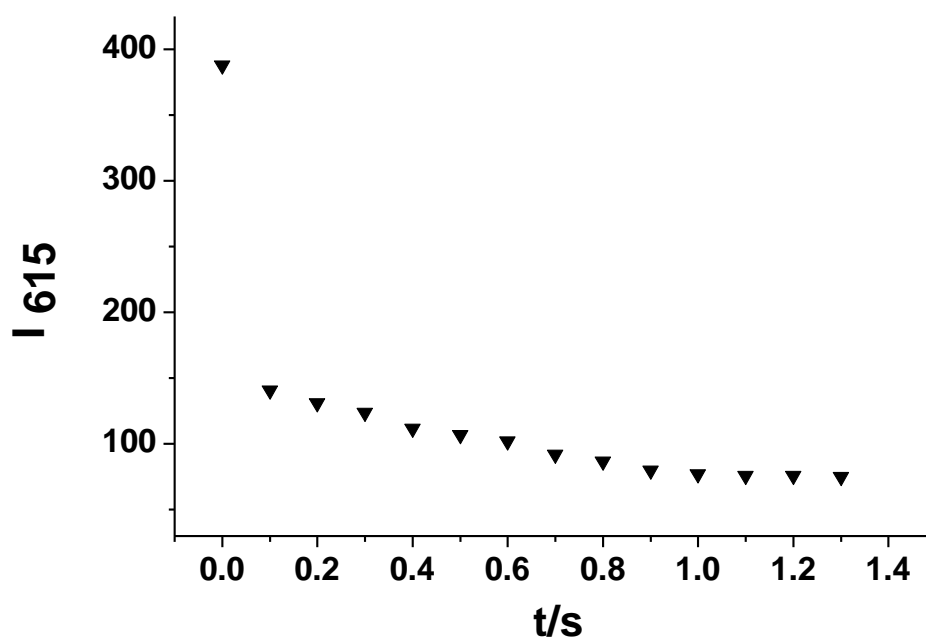


**Fig. S22.** The time-dependent behavior of chemosensor **3** in aqueous media upon addition of 6.0 equivalent cyanide ions.

14. Fluorescence spectra of chemosensor **3** in the presence of different cations in H<sub>2</sub>O

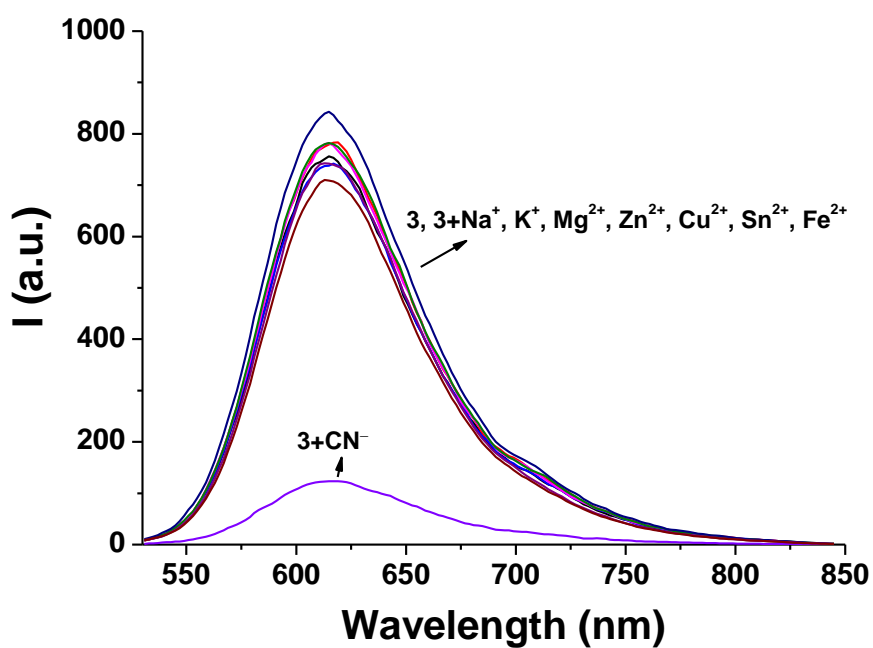


**Fig. S23.** Fluorescence intensity changes of **3** with other heavy metal ions. Fluorescence spectra (excitation at 515 nm) of **3** ( $20 \mu\text{mol L}^{-1}$ ) with 6.0 equivalents of various metal ions (NaCl, KCl, KI,  $\text{CuSO}_4 \cdot 5\text{H}_2\text{O}$ ,  $\text{ZnCl}_2$ ,  $\text{MgSO}_4 \cdot 7\text{H}_2\text{O}$ ,  $\text{FeSO}_4 \cdot 7\text{H}_2\text{O}$ ,  $\text{SnCl}_2$ , TBACN) were recorded in DMSO/H<sub>2</sub>O (1:1 v/v).

15. Linear fluorescence response of chemosensor **3** to  $\text{CN}^-$  in DMSO/ $\text{H}_2\text{O}$

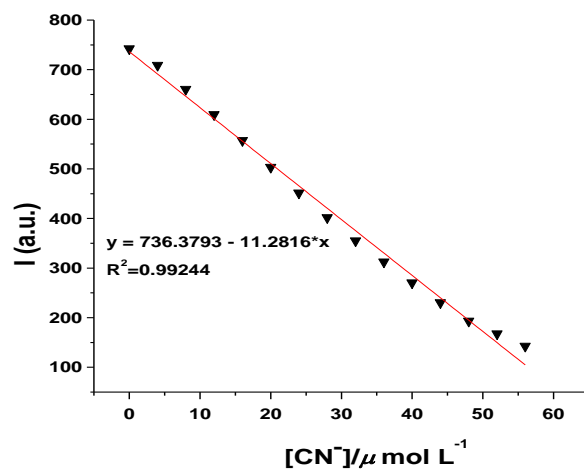


**Fig. S24.** Linear fluorescence response of chemosensor **3** to  $\text{CN}^-$  concentration ranging from 0 to  $56 \mu\text{mol L}^{-1}$  (0-2.8 equiv) in DMSO/ $\text{H}_2\text{O}$  (1:1, v/v).

16. The fluorescence detection limit of the chemosensor **3** with  $\text{CN}^-$  in DMSO.

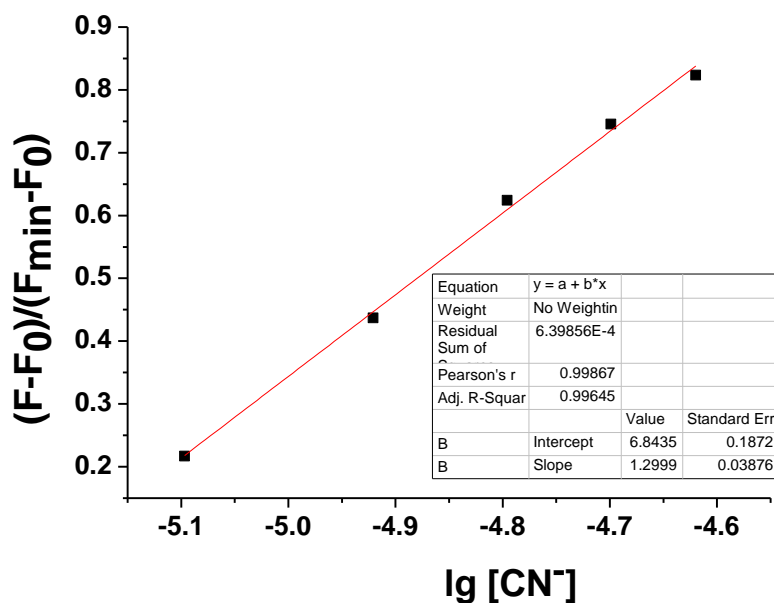


**Fig. S25.** Response of fluorescence intensity to changing  $\text{CN}^-$  concentrations in DMSO. ( $[\mathbf{3}] = 20 \mu\text{mol L}^{-1}$ ,  $[\text{CN}^-] = 5000 \mu\text{mol L}^{-1}$ ,  $\lambda_{\text{ex}} = 515 \text{ nm}$ ,  $\lambda_{\text{em}} = 520 \text{ nm}$ ).

The result of the analysis as follows:

Linear Equation:  $y = 6.8435 + 1.2999 \cdot x$ ,  $R^2 = 0.99645$

$\text{LOD} = K \cdot \delta/S = 0.034 \mu\text{mol L}^{-1}$

17. The fluorescence detection limit of the chemosensor **3** with  $\text{CN}^-$  in DMSO/ $\text{H}_2\text{O}$ .

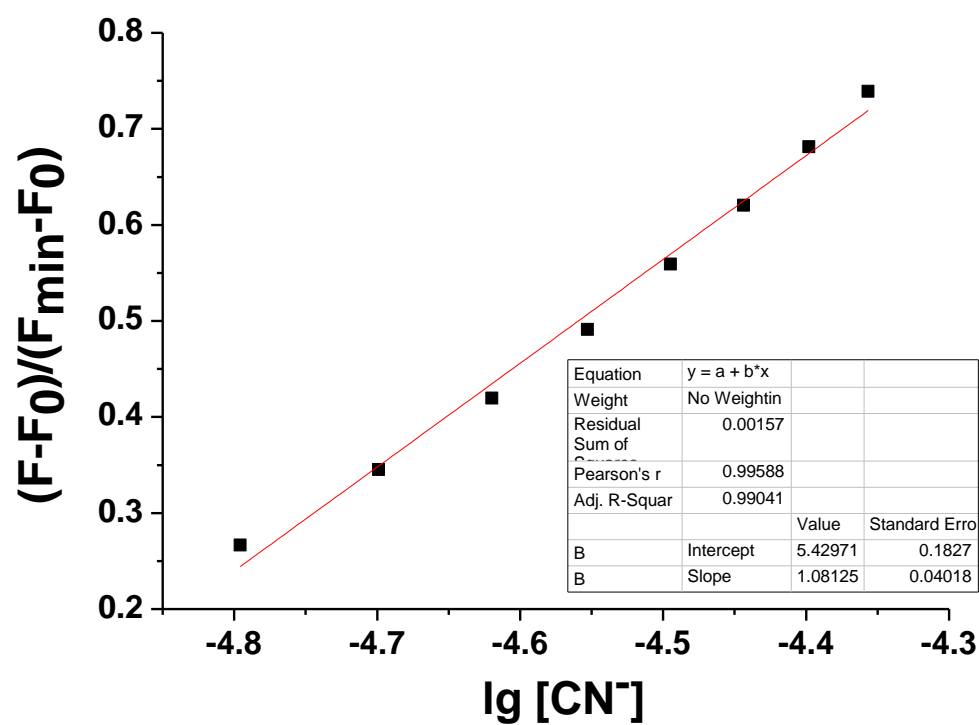


**Fig. S26.** Response of fluorescence intensity to changing  $\text{CN}^-$  concentrations in DMSO/ $\text{H}_2\text{O}$  (1:1,  $v/v$ ). ( $[\mathbf{3}] = 20 \mu\text{mol L}^{-1}$ ,  $[\text{CN}^-] = 5000 \mu\text{mol L}^{-1}$ ,  $\lambda_{\text{ex}} = 515 \text{ nm}$ ,  $\lambda_{\text{em}} = 525 \text{ nm}$ ).

The result of the analysis as follows:

Linear Equation:  $y = 5.42971 + 1.08125 \cdot x$ ,  $R^2 = 0.99041$

$\text{LOD} = K \cdot \delta/S = 0.045 \mu\text{mol L}^{-1}$

18. The fluorescence detection limit of the chemosensor **3** with  $\text{CN}^-$  in  $\text{H}_2\text{O}$ .

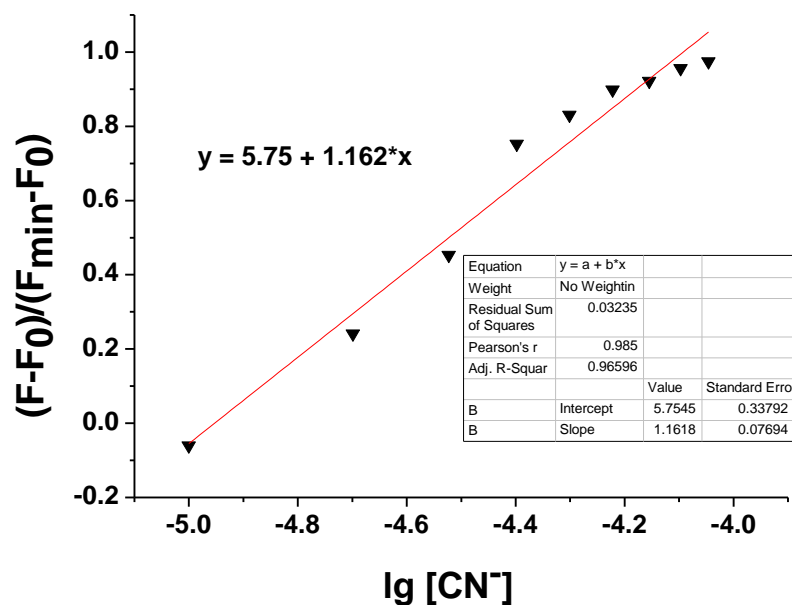


**Fig. S27.** Response of fluorescence intensity to changing  $\text{CN}^-$  concentrations in  $\text{H}_2\text{O}$ . ( $[\mathbf{3}] = 20 \mu\text{mol L}^{-1}$ ,  $[\text{CN}^-] = 5000 \mu\text{mol L}^{-1}$ ,  $\lambda_{\text{ex}} = 480 \text{ nm}$ ,  $\lambda_{\text{em}} = 500 \text{ nm}$ ).

SD	N
0.06798	9

The result of the analysis as follows:

Linear Equation:  $y = 5.75 + 1.162 * x$ ,  $R^2 = 0.96596$

$S = 1.16 * 10^6$ ,  $K = 3$ ,  $\delta = 0.06798$

$\text{LOD} = K * \delta/S = 0.18 \mu\text{mol L}^{-1}$

19. The  $^1\text{H}$  NMR spectra of the chemosensor **3** with  $\text{CN}^-$  in  $\text{DMSO-}d_6$ .

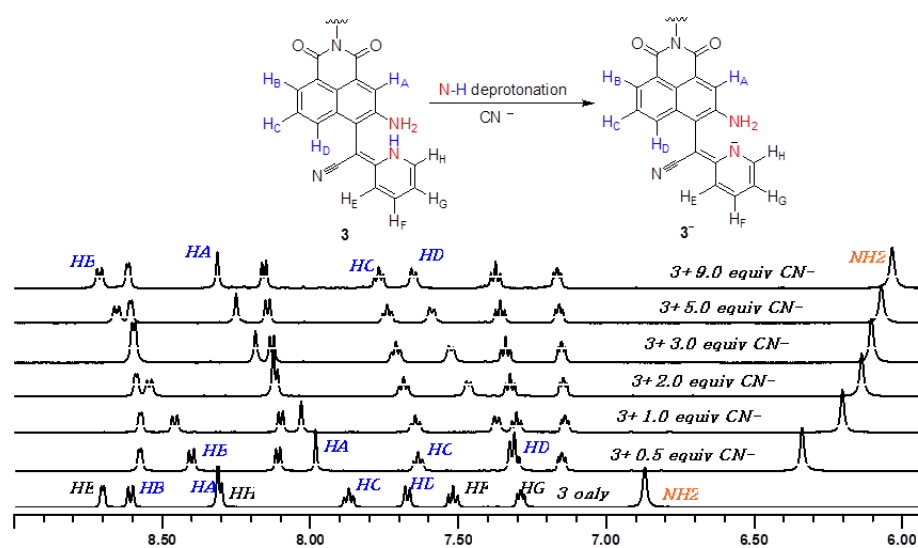


**Fig. S28.**  $^1\text{H}$ -NMR titration spectra of chemosensor **3** ( $4.0 \times 10^{-2}$  mol L<sup>-1</sup>) in  $\text{DMSO-}d_6$  upon addition of  $\text{CN}^-$  ions (as TBA salts in  $\text{DMSO-}d_6$ ) at 298 K.

20. The  $^1\text{H}$  NMR spectra of the chemosensor **3** with  $\text{F}^-$  in  $\text{DMSO-}d_6$ .

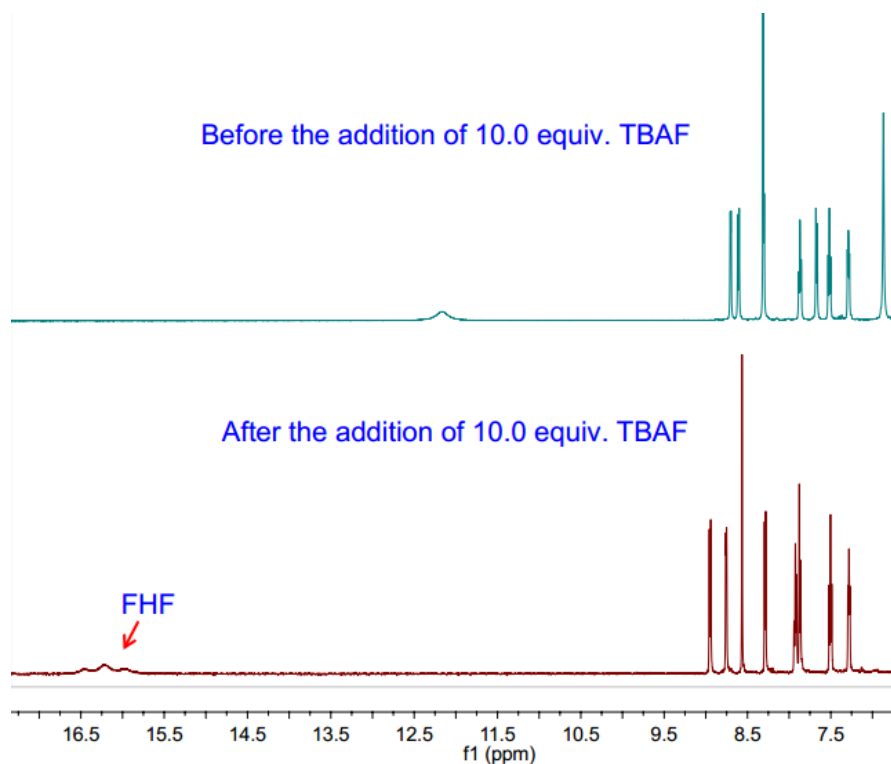


**Fig. S29.** The  $^1\text{H}$  NMR spectra of the chemosensor **3** ( $0.04$  mol L<sup>-1</sup>) followed by the addition of 10.0 equiv. TBAF in  $\text{DMSO-}d_6$ .

21. Confocal microscopic images of HeLa cells.

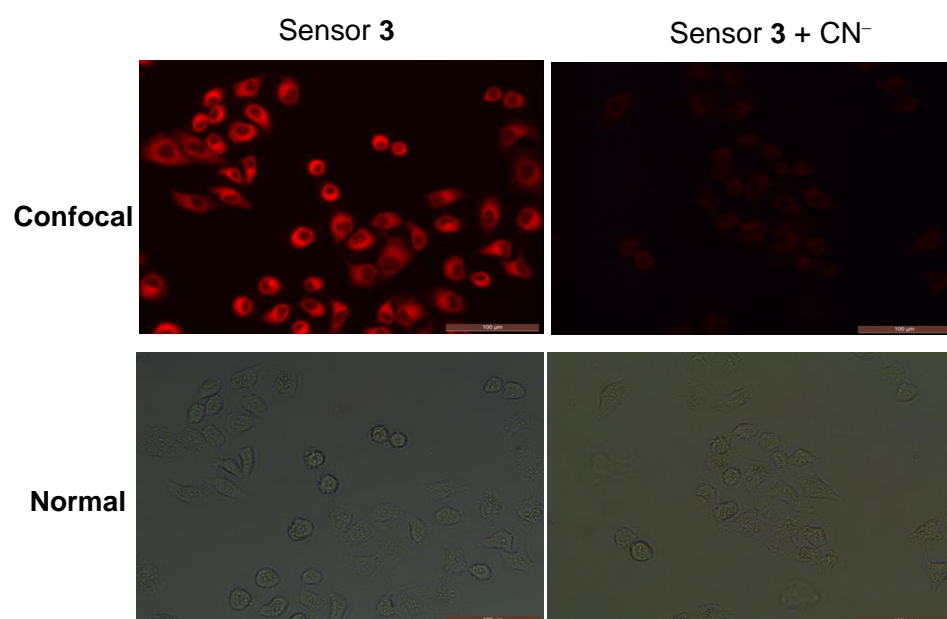


**Fig. S30.** Confocal fluorescence microscope images of HeLa cells in the presence of chemosensor **3** ( $10 \mu\text{mol L}^{-1}$ ). The fluorescence images were recorded after 10 min of treatment of  $\text{CN}^-$  ( $10 \mu\text{mol L}^{-1}$ ) at  $37^\circ\text{C}$ .

22. Fluorescence spectra of chemosensor **3** at different pH values in DMSO/ $\text{H}_2\text{O}$ .

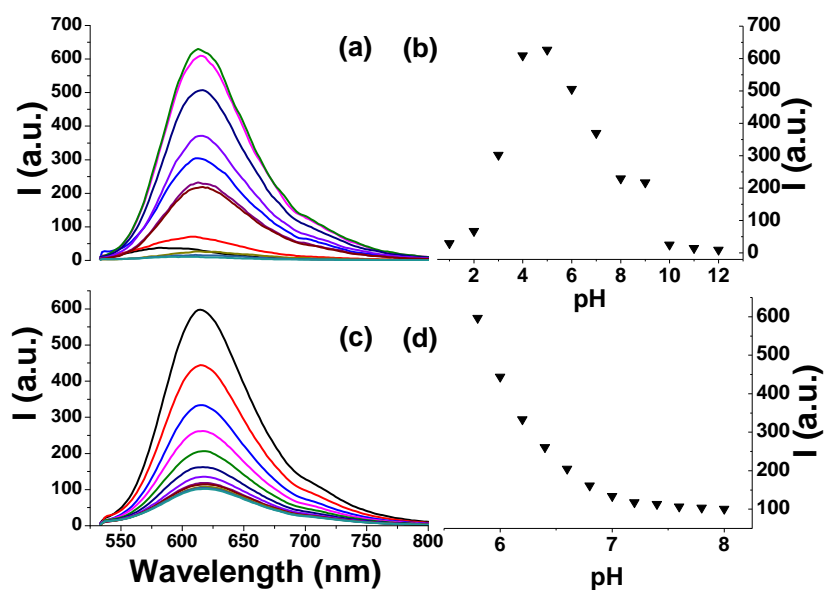
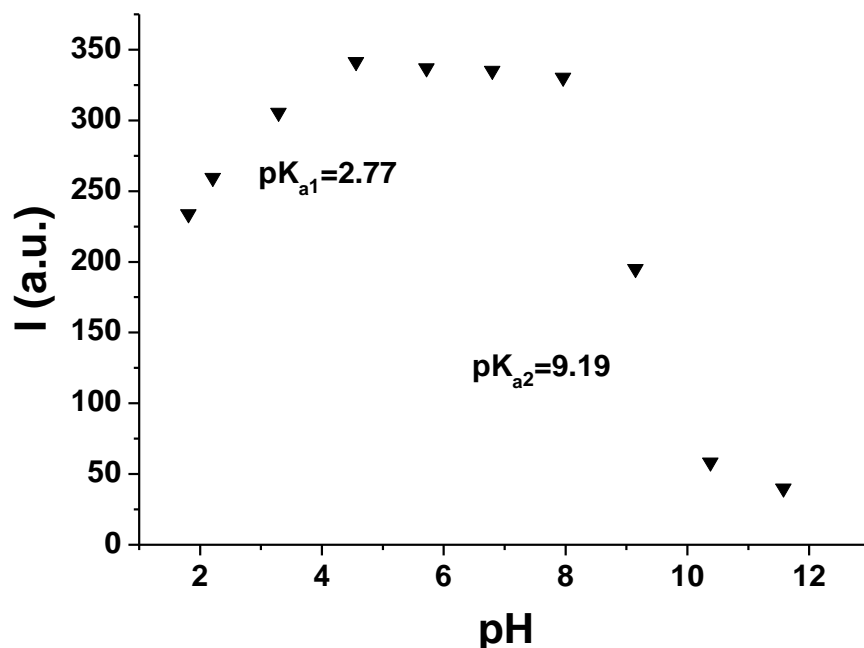


**Fig. S31.** Fluorescence spectra of chemosensor **3** at different pH values (515 nm excitation) in DMSO/ $\text{H}_2\text{O}$  (1:1) ranging from (a) 1–14, (c) 5.8–8.0. (b) Relationship between the pH and the fluorescence intensity at 615nm ranging from (b) 1–14, (d) 5.8–8.0.



23. Fluorescence spectra of chemosensor **3** at different pH values in H<sub>2</sub>O.



Typical procedure of the  $pK_a$  value obtained:  $\log[(F_{max}-F)/(F-F_{min})]=pK_a-pH$ , where  $F$  is the fluorescence emission intensity at 618 nm.

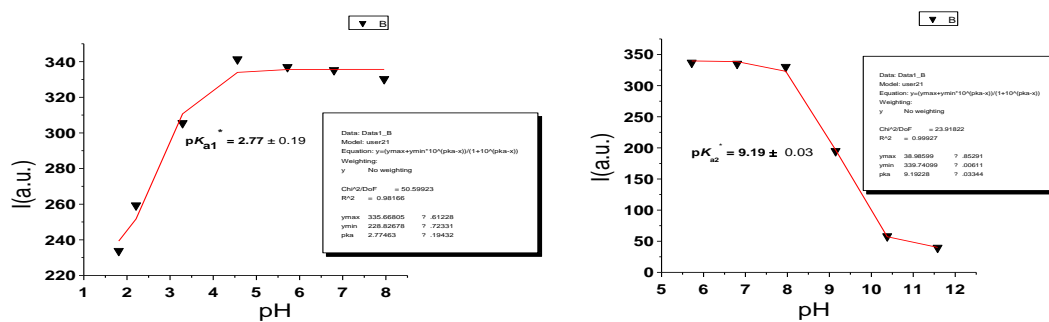


**Fig. S32.** Relative intensity of **3** at 618 nm in Britton-Robinson buffer solution as a function of pH,  $pK_{a1}$  and  $pK_{a2}$  values are calculated.